Journal of Nuclear Materials 377 (2008) 132–135

Contents lists available at ScienceDirect

Journal of Nuclear Materials

journal homepage: www.elsevier.com/locate/jnucmat

Reaction kinetics analysis of damage evolution in accelerator driven system beam windows

T. Yoshiie [a,*], Q. Xu [a], K. Sato [a], K. Kikuchi [b], M. Kawai [c]

[a] Research Reactor Institute, Kyoto University, Kumatori-cho, Sennan-gun, Osaka-fu 590-0494, Japan
[b] Japan Atomic Energy Agency, Tokai-mura, Naka-gun, Ibaraki-ken 319-1195, Japan
[c] High Energy Accelerator Research Organization, Oho, Tsukuba-shi, Ibaraki-ken 305-0801, Japan

A B S T R A C T

Reaction kinetic analysis was used to estimate the damage evolution in window materials of 800 MWth accelerator driven system (ADS). Parameters were fitted to F82H of the STIP-II experiment at 673 K and EC316LN of the STIP-I experiment at 626 K. In F82H, the concentration of bubbles was almost constant and the bubble size increased, while the concentration of interstitial type dislocation loops increased and their size was constant between 2.1×10^{-3} and 210 dpa. EC316LN showed almost the same behavior. Swelling increased almost linearly with irradiation dose above 0.21 dpa between 673 K and 773 K.

1. Introduction

An accelerator driven system (ADS) is a coupling of a subcritical nuclear reactor with a proton accelerator. High energy protons irradiated in a liquid metal target produce a large number of neutrons. These neutrons are used to transmute minor actinide in high level waste from light water reactor fuels. The beam window of ADS is thus subjected to a very high irradiation load by source protons and spallation neutrons as well as neutrons generated inside the reactor. At present, there are no materials that enable the window to be operational for the desired period of time without deterioration of mechanical properties.

Irradiation experiments are essential for the development of nuclear materials. However, there are several cases in which, materials are developed without appropriate irradiation facilities, such as fusion reactor materials and high intensity spallation neutron source target related materials. In these cases, computer simulations play an important role in predicting materials behavior. Reaction kinetics analysis using rate equations is a powerful technique for predicting defect evolution from the initial stage of irradiation (nucleation of defect clusters) to large defect cluster formation (growth of defect clusters) [1,2].

Ferritic stainless steels such as F82H and austenitic stainless steels such as type 316 are regarded as candidate materials for the beam window. In this paper, the growth of defect structures in proton-irradiated austenitic stainless steel (EC316LN) and ferritic martensitic stainless steel (F82H) is investigated through reaction kinetics analysis assumed an ADS beam window of 800 MWth, which is designed in Japan for the transmutation of long-living nuclear isotopes in spent fuel, with a proton energy of 1.5 GeV and liquid Pb–Bi for spallation target and coolant [3].

2. Outline of the model

The irradiation conditions for the 800 MWth ADS beam window are tabulated in Table 1. The variation in point defects, defect clusters and helium concentrations, and growth of point defect clusters were calculated using the dynamic rate theory. As the irradiation temperature is high, the effect of hydrogen on the evolution of defect structure was ignored. Oliver et al. have observed the helium release stage at 1000 K in STIP-1 irradiated SS316L and assigned it to the release of helium from bubbles [4]. Thus, this model did not incorporate the interaction of helium with interstitials and interstitial clusters (interstitial type dislocation loops). High primary knock-on energies deposited in materials are one of the significant differences between a high energy proton plus generated neutron spectrum and a fission neutron spectrum. We have studied the effect of neutron spectrum between fission and fusion neutrons on the evolution of defect structure [5]. In metals with heavy atoms such as Au, the effect of cascade size on the damage structure is significant. In metals with intermediate weight atoms such as Ni, the effect of cascade size is attributed to the number of subcascades. This number is proportional to the primary knock-on energies. The generation of point defects and the nucleation of point defect clusters occur in each subcascade. Thus, the effect of the large primary knock-on energies was introduced as the direct formation of point defect clusters. Recently, the importance of moving interstitial clusters in metals for void growth have been pointed out [6]. Most of observations were, however, performed in pure metals and it was shown that alloying elements prevent the motion [7]. As it is unclear whether or not the movement

* Corresponding author. Tel.: +81 724 51 2473; fax: +81 724 51 2620.
E-mail address: yoshiie@rri.kyoto-u.ac.jp (T. Yoshiie).

0022-3115/$ - see front matter © 2008 Elsevier B.V. All rights reserved.
doi:10.1016/j.jnucmat.2008.02.059

Table 1
Irradiation conditions of 800 MWth ASD beam window

Irradiation temperature	723 K (center)–773 K (near perimeter)
Damage rate	2.12×10^{-6} dpa/s
He production rate	3.68×10^{-11} He/s

occurs in practical alloys such as ferittic/martenstic steels, we did not consider interstitial clusters as mobile defects.

Other assumptions used in the calculation were as follows:

(1) The damage due to protons and neutrons, and the effect of helium are considered simultaneously.
(2) Only helium, interstitials and vacancies are mobile.
(3) As defect clusters, vacancy-helium pairs, vacancy clusters (voids), vacancy clusters with helium (bubbles) and interstitial clusters (interstitial type dislocation loops) are considered. Vacancy-helium pair, one helium in one vacancy, is not included in bubbles, since it is not possible to observe by electron microscopy.
(4) Thermal dissociation is considered for vacancy-helium pairs.
(5) Di-interstitials and di-vacancies are set for stable nuclei of clusters [1].
(6) Nuclei of interstitial clusters and vacancy clusters are also formed directly in cascades.
(7) Materials parameters used for austenitic stainless steels and ferritic stainless steels are those for Ni and Fe, respectively.
(8) The irradiation temperatures of ADS target materials are from 673 K to 723 K.

The concentrations of interstitials (C_I), vacancies (C_V), and helium (C_{He}) are expressed as

$$\frac{dC_I}{dt} = P_I - 2Z_{I,I}M_IC_I^2 - Z_{I,V}(M_I + M_V)C_IC_V - Z_{I,IC}M_IC_IS_I - Z_{I,VC}M_IC_IS_V - Z_{I,B}M_IC_IS_B - Z_{I,VHe}M_IC_IC_{V,He} - M_IC_IC_S - N_IP_{IC},$$

$$\frac{dC_V}{dt} = P_V - 2Z_{V,V}M_VC_V^2 - Z_{I,V}(M_I + M_V)C_IC_V - Z_{He,V}M_{He}C_VC_{He} - Z_{V,V}M_VC_VS_V - Z_{V,IC}M_VC_VS_I - Z_{V,B}M_VC_VS_B - Z_{V,He}M_VC_VC_{He} - Z_{V,He}M_VC_VC_{V,He} + M_{He}T_{V,He}C_{V,He} + Z_{I,VHe}M_IC_IC_{V,He} - M_VC_VC_S - N_VP_{VC},$$

$$\frac{dC_{He}}{dt} = P_{He} - Z_{He,V}M_{He}C_VC_{He} - Z_{He,V}M_{He}C_{He}S_V - Z_{He,B}M_{He}C_{He}S_B - Z_{He,V}M_{He}C_{He}C_{V,He} + Z_{I,VHe}M_IC_IC_{V,He} + M_{He}T_{V,He}C_{V,He} - M_{He}C_{He}C_S,$$

where P is the production rate of Frenkel pairs, and Z is the number of sites of the spontaneous reaction of each process. M is the mobility of defects and expressed as $\nu \exp\left(-\frac{E}{kT}\right)$, where ν is the jump frequency. E, k and T are the migration energy, the Boltzmann constant and temperature, respectively. S is the sink efficiency to mobile defects and expressed as [1,2]:

$$S_V = (48\pi^2 R_V C_{VC}^2)^{1/3},$$
$$S_I = 2(\pi R_I C_{IC})^{1/2},$$
$$S_B = (48\pi^2 R_{V,He} C_B^2)^{1/3}.$$

N is the number of atoms in clusters formed directly in cascades, T is the probability of dissociation of helium from a vacancy. The subscripts I, V, IC, VC, B and He denote interstitials, vacancies, interstitial type dislocation loops, voids, bubbles and He, respectively. The concentrations are fractional units.

The nucleation rates of interstitial type dislocation loops (concentration, C_{IC}), voids (C_{VC}), vacancy-He pairs ($C_{V,He}$), and bubbles (C_B) are

$$\frac{dC_{IC}}{dt} = P_{IC} + Z_{I,I}M_IC_I^2,$$
$$\frac{dC_{VC}}{dt} = P_{VC} + Z_{V,V}M_VC_V^2 - M_{He}C_{He}S_V,$$
$$\frac{dC_{V,He}}{dt} = Z_{He,V}M_{He}C_V - Z_{V,VHe}M_VC_VC_{V,He} - Z_{I,VHe}M_IC_IC_{V,He} - M_{He}T_{V,He}C_{V,He} - ZM_{He}C_{He}C_{V,He},$$
$$\frac{dC_B}{dt} = Z_{V,He}M_VC_VC_{V,He} - Z_{He,VC}M_{He}C_{He}C_{VC} + Z_{He,VHe}M_{He}C_{He}C_{V,He}.$$

P_{IC} and P_{VC} are the production rates of interstitial type dislocation loops and voids directly from cascades.

The total accumulation of interstitials in loops (R_I) and that of vacancies in voids (R_V) and in bubbles (R_B) are

$$\frac{dR_I}{dt} = Z_{I,IC}M_IC_IS_I - Z_{V,IC}M_VC_VS_I + N_IP_{IC}$$
$$\frac{dR_V}{dt} = Z_{V,VC}M_VC_VS_V - Z_{I,VC}M_IC_IS_V + N_VP_{VC} - Z_{He,VC}M_{He}C_{He}S_V \times \frac{R_V}{C_{VC}},$$
$$\frac{dR_B}{dt} = Z_{V,B}M_VC_VS_B - Z_{I,B}M_IC_IS_B + Z_{He,VC}M_{He}C_{He}S_V \times \frac{R_V}{C_{VC}} + Z_{He,VHe}M_{He}C_{He}C_{V,He}.$$

3. Results and discussion

As initial values of parameters, values in a book of Damask and Dienes [8] were used and changed to fit two experimental results for ferritic martensitic steel F82H irradiated in STIP-II [9], and solution-annealed austenitic steel EC316LN in STIP-I [10] as shown in Table 2. Defect clusters in F82H by STIP-II irradiation were set to interstitial type dislocation loops. Fig. 1 shows the variation in loop and bubble concentrations, and loop and bubble diameters in F82H with the irradiation conditions of STIP-II. The parameters determined are tabulated in Table 3. Parameters marked with '*' are adjusted for fitting. The computational results match so well with the experimental values at about 10 dpa. It is due to the fact that in our model the concentration of clusters is mainly determined by P_{IC} and P_{VC} and the growth of clusters is by the size of reaction sites such as $Z_{I,IC}$ and $Z_{V,IC}$. Using the same parameters, defect cluster evolution was calculated with ADS conditions. Fig. 2 compares the defect structures obtained under the STIP-II conditions and ADS conditions at 673 K. The concentration of loops and bubbles is not very different, however, the size of bubbles is larger and the size of loops is smaller under STIP-II conditions. This was caused by the difference in damage rate and helium production rate.

The change of interstitial, vacancy and helium concentrations under ASD conditions at 723 K is shown in Fig. 3. At first, the

Table 2
Irradiation conditions and transmission electron microscopy results

Specimen	Dose (dpa)	He (appm)	Tirr (K)	Loops		Bubbles	
				Mean size (nm)	Density (m^{-3})	Mean size (nm)	Density (m^{-3})
EC316LN [10]	11	730	626 ± 28	15.9	3.6×10^{22}	1.6	5.3×10^{23}
F82H [9]	20.3	1800	673 ± 50	8.5	2.88×10^{22}	5.0	2.48×10^{23}

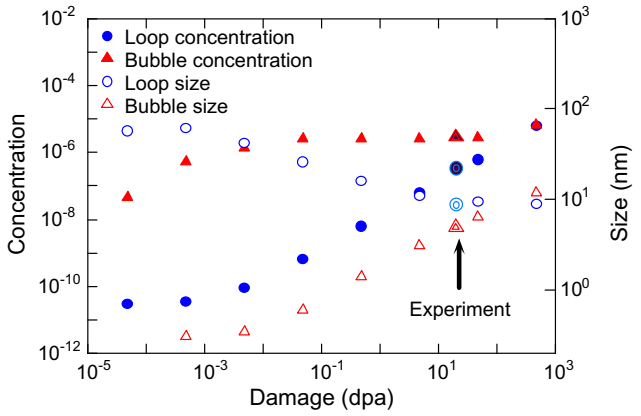

Fig. 1. Simulation of the evolution of defect structure in F82H irradiated by STIP-II at 673 K. Experimental data indicated by the arrow are results by Jia and Dai [9].

Table 3
Parameters used in simulation

	EC316L	F82H
$^*P_{IC}$	$5.1 \times 10^{-7} \times P$	$1.3 \times 10^{-8} \times P$
$^*P_{VC}$	$0.4 \times 10^{-7} \times P$	$1.0 \times 10^{-8} \times P$
E_M^I	0.15 [11]	0.26 eV [12]
E_M^V	1.0 [13]	1.24 eV [12]
E_M^{He}	0.06 [14]	0.08 [15]
$E_B^{V\text{-}He}$	3.2 [16]	3.9 [16]
C_S	10^{-10}	10^{-10}
C_{SHe}	10^{-15}	10^{-15}
$^*Z_{IV}$	84.0	45.0
$^*Z_{II}$	1.1	1.0
$^*Z_{VV}$	1.1	0.15
$^*Z_{I,VC}$	40.5	40.4
$^*Z_{V,VC}$, $^*Z_{V,B}$, $^*Z_{I,B}$	40.0	40.0
$^*Z_{He,VC}$	25.5	27.0
N_I, N_V	10.0	10.0
ν	$10^{-13} s^{-1}$	10^{-13} s^{-1}

*: Parameters to fit experiments.
P: Production rate of point defects.

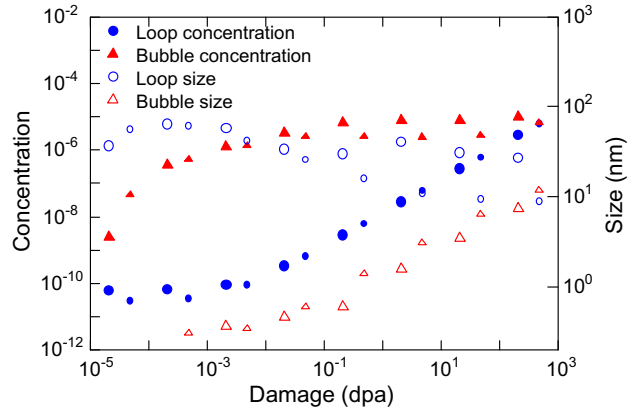

Fig. 2. Comparison of STIP-II (small symbol) and ADS (large symbol) irradiations in F82H at 673 K.

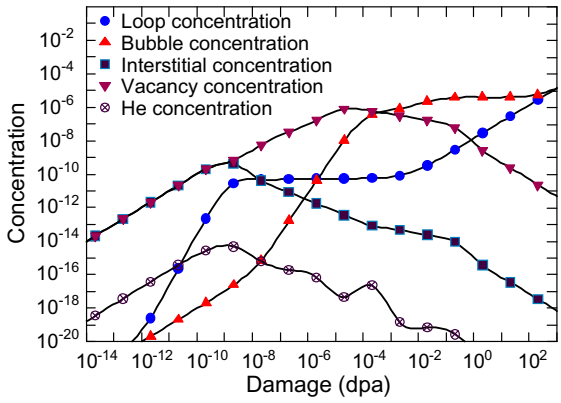

Fig. 3. Behavior of point defects and their clusters and helium in F82H at 723 K by ADS irradiation.

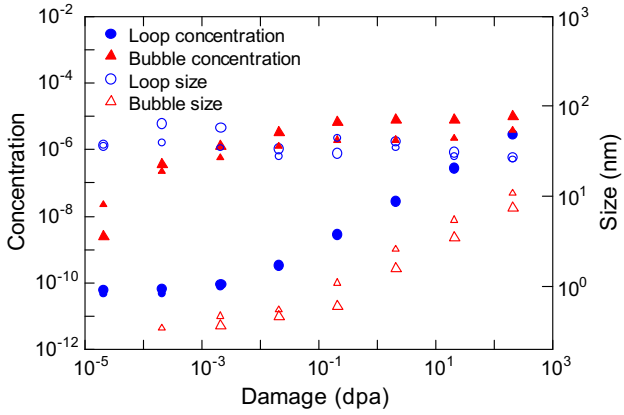

Fig. 4. The effect of irradiation temperature in F82H between 673 K (large symbol) and 773 K (small symbol) by ADS irradiation. Loop concentrations are almost the same between two temperatures.

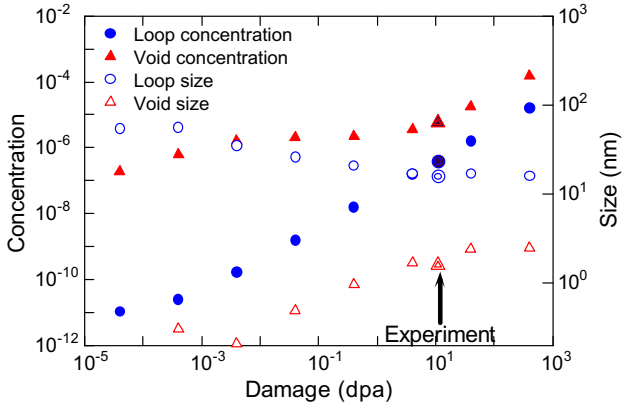

Fig. 5. Simulation of evolution of defect structure in EC316LN irradiated by STIP-I at 626 K. Experimental data indicated by arrow are results by Hamaguchi and Dai [10].

concentrations of interstitials and vacancies increase with irradiation time. Then, as the mobility of interstitials is high, the concentration of interstitials starts to decrease owing to their absorption by permanent sinks and point defect clusters. The loop size is large because of high interstitial concentration at low dose. The concentration of interstitial type dislocation loops is constant since most loop nuclei are formed by di-interstitials. The increase in loop concentration, which starts in the later stages of irradiation ($>10^{-2}$ dpa), is caused by the direct formation of loops in cascades. From the dose of 10^{-4} dpa, the vacancy concentration starts to decrease owing to the low mobility of vacancies. At the same time, the bubble concentration stops increasing and the bubble size starts to increase (see Fig. 2). The temperature dependence of the

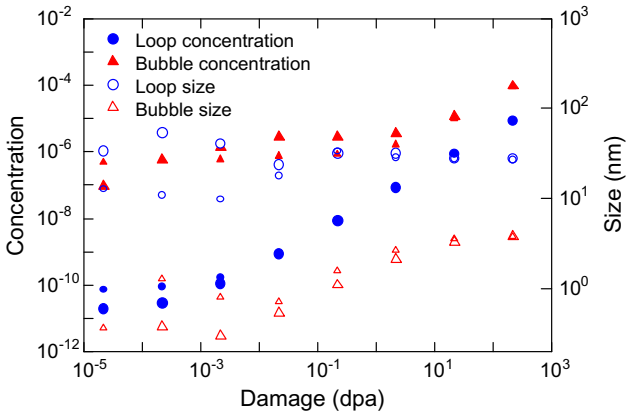

Fig. 6. The effect of irradiation temperature in EC316LN between 673 K (large symbol) and 773 K (small symbol) by ADS irradiation.

Table 4
The estimated swelling in F82H and EC316LN at three different temperatures

	Temp. (K)	2.1 dpa (%)	21 dpa (%)	210 dpa (%)
F82H	673	0.13	1.5	15
	723	0.15	1.5	15
	773	0.15	1.5	15
316LN	673	0.13	1.0	9.6
	723	0.14	1.1	9.8
	773	0.11	0.97	9.5

evolution of defect structure at 673 K and 773 K is shown in Fig. 4. At higher dose, the loop concentration and size are almost the same. The bubble concentration is lower and the bubble size is higher at higher temperatures.

The change of loop and bubble concentrations and loop and bubble diameters in EC316LN under the irradiation conditions of STIP-I is shown in Fig. 5 along with experimental results. The parameters determined are tabulated in Table 3. The evolution of defect structure at 673 K and 773 K under ADS conditions is shown in Fig. 6. At higher doses, the defect concentration and size are almost the same for the two temperatures.

Table 4 tabulates the swelling in F82H and EC316NL at three different temperatures. In both alloys, the swelling is almost proportional to the dose, indicating the steady-state growth region. The swelling of austenitic stainless steel EC316LN is relatively low compared to that of ferritic martensitic steel F82H. It is generally believed that the swelling of fcc metals is higher than that of bcc metals because of the high dislocation bias factor. One possible explanation is that the parameter fitting in EC316LN was performed using the experimental data for 626 K and the temperature dependence of the evolution of defect structure was not expressed well in our model. Another possibility is that the effect of bias factor is insignificant under damage evolution with high dose protons since there are differences in the evolution of defect structure between fission neutron irradiation and proton irradiation. More experimental results are required for high dose proton irradiation at high temperature.

4. Conclusion

Reaction kinetic analysis was used to estimate the evolution of the damage structure of F82H and EC316LN under 800 MWth ASD conditions. Parameters were fitted by STIP experiments. The two alloys showed almost the same behavior between 2.1×10^{-3} and 210 dpa. The concentration of bubbles was almost constant and the bubble size increased, while the concentration of interstitial type dislocation loops increased and their size remained constant. The swelling increased almost linearly with irradiation dose between 673 K and 773 K, indicating the steady-state growth region of bubbles with irradiation damage.

References

[1] N. Yoshida, M. Kiritani, J. Phys. Soc. Jpn. 35 (1973) 1418.
[2] T. Yoshiie, S. Kojima, Y. Satoh, K. Hamada, M. Kiritani, J. Nucl. Mater. 191–194 (1992) 1160.
[3] K. Nishihara, K. Kikuchi, J. Nucl. Mater. 377 (2008) 298.
[4] B.M. Oliver, Y. Dai, R.A. Causey, J. Nucl. Mater. 356 (2006) 148.
[5] T. Yoshiie, Y. Satoh, Q. Xu, J. Nucl. Mater. 329–333 (2004) 81.
[6] B.N. Singh, H. Trinkaus, C.H. Woo, J. Nucl. Mater. 212–215 (1994) 168.
[7] T. Yoshiie, Mater. Trans. 46 (2005) 425.
[8] A.C. Damask, G.J. Dienes, Point Defects in Metals Gordon and Breach, Science Publishers, Inc., 1963.
[9] X. Jia, Y. Dai, J. Nucl. Mater. 356 (2006) 105.
[10] D. Hamaguchi, Y. Dai, J. Nucl. Mater. 343 (2005) 262.
[11] T. Yoshiie, S. Kojima, Y. Satoh, K. Hamada, M. Kiritani, J. Nucl. Mater. 191–194 (1992) 1160.
[12] M. Kiritani, H. Takata, K. Moriyama, F.E. Fujita, Philos. Mag. A 40 (1979) 779.
[13] M. Kiritani, M. Konno, T. Yoshiie, S. Kojima, Mater. Sci. Forum 15–18 (1987) 181.
[14] C.C. Fu, F. Willaime, Phys. Rev. B 72 (1–6) (2005) 064117.
[15] K. Morishita, R. Sugano, B.D. Wirth, J. Nucl. Mater. 323 (2003) 243.
[16] D.J. Reed, Radiat. Eff. 31 (1977) 129.